SIMPLE MAGNETOSTATIC DELAY LINES*

Michael R. Daniel and J. D. Adam
Westinghouse Electric Corporation
Research & Development Center
Pittsburgh, PA 15235

ABSTRACT

We describe, through calculation and experiment, how simple, single finger, microstrip transducers may be used to demonstrate both linearly dispersive and constant delay type magnetostatic delay lines. The desired delay behavior is achieved over some useful measure of bandwidth through the influence of a close proximity ground plane to the yttrium iron garnet film. The two limitations of this technique are pointed out and one possible remedy to one of them is shown.

1. INTRODUCTION

The promise of magnetostatic waves as delay line elements at microwave frequencies rests on their strong electromagnetic coupling to transducers and their low propagation losses in films of yttrium iron garnet (YIG). However, the implementation of either a constant delay or a linearly dispersive delay versus frequency characteristic is governed by the need to modify the inherently non-linear dispersion which magnetostatic waves show in general. The very successful exploitation of the interdigital transducer and the reflective array

*Work supported in part by United States Air Force (RADC) under Contract No. F19628-80-C-0150, and also in part by the U.S. Air Force Avionics Laboratory under Contract No. F 33615-77-C-1068.

for surface acoustic wave (SAW) devices rests on the weak coupling which these waves have. Thus, the strong coupling magnetostatic waves have not, so far, been able to take advantage of these tools for delay line design except with a very limited number of finger pairs. But photolithographic limitations and transducer losses limit SAW devices to an upper frequency of around 1 GHz whereas magnetostatic devices have relaxed photolithographic requirements and, in YIG films, an upper frequency limit of around 20 GHz. There was, thus, a strong motivation for, temporarily at least, bypassing the high coupling problems and examining the possible exploitation of simple single finger transducers on single YIG films. The problem of controlling the dispersion was addressed by recognizing the strong influence of a close proximity ground plane on the magnetostatic wave delay time.

2. EXPERIMENTAL RESULTS AND CALCULATIONS

Figure 1 shows the geometry of the simple delay line together with the static bias field orientations required to launch each of the three magnetostatic wave types. The single finger transducers are typically 2 mils (50 μm) wide defined photolithographically in 5 μm thick gold. The ground plane spacing can be controlled by the alumina substrate thickness. Examples of the delay performance which can be obtained using forward volume waves (FVW's) are shown in Figure 2. In the upper, dispersive delay curve, a 20 μm thick YIG film was placed 20 μm from a ground plane resulting in delay versus frequency response linear to within ± 5 nS over 1.2 GHz of bandwidth. This particular delay line has already been referred to in the first paper of this session. It is presently being evaluated by Westinghouse in both the

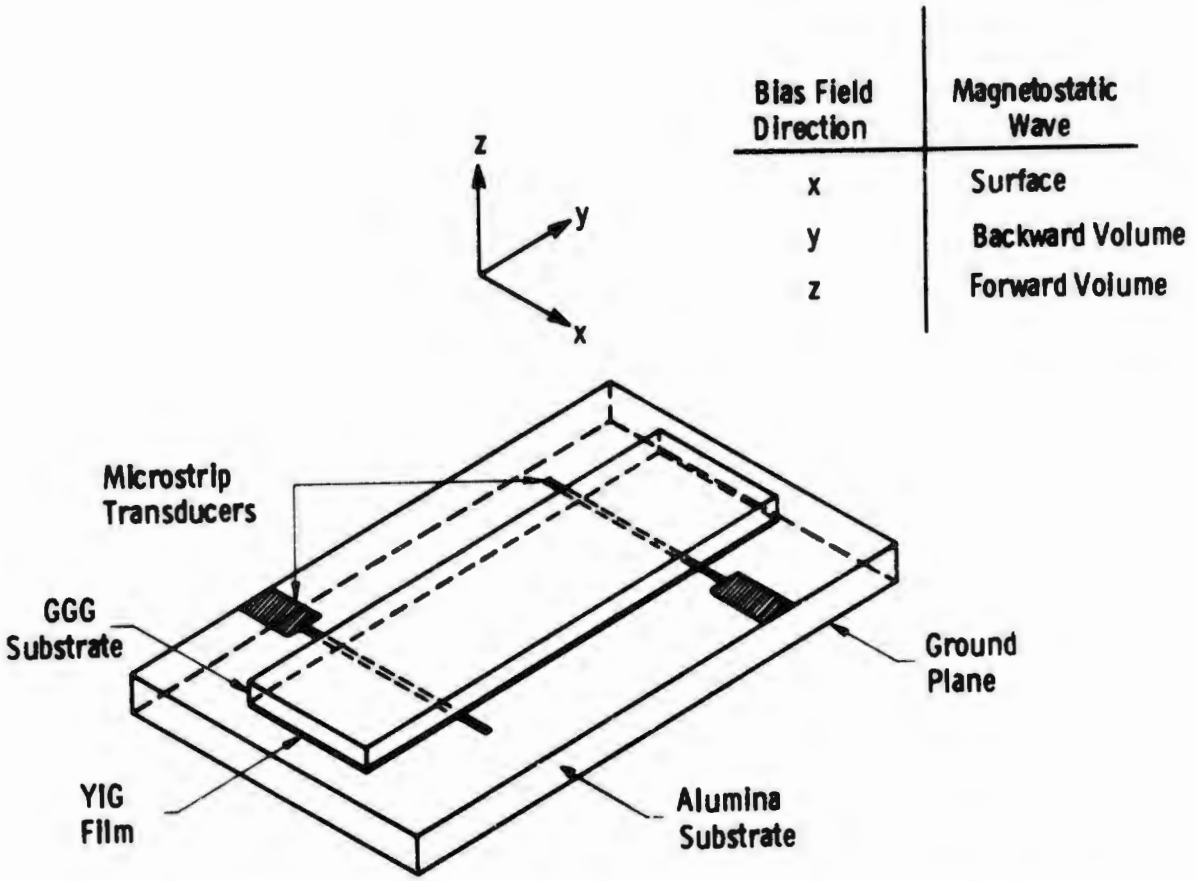

Figure 1. Magnetostatic delay line configuration with the inset at top right showing the magnetic bias field directions required to launch each of the three magnetostatic wave types.

X-band and S-band versions as the dispersive delay element in a microscan receiver. The unmatched insertion loss was in the range 35 to 40 dB over the active bandwidth. This relatively high value for magnetostatic waves was also commented on in the first paper and represents the price to be paid for simplicity of design using the close ground plane technqiue. Depending on the closeness of this plane to the YIG surface some measure of increased insertion loss will always be experienced due to finite conductivity damping of the magnetostatic wave by the ground plane. The lower curve of Figure 2 shows a delay response constant to within a ± 5 nS tolerance. Achieving

a constant delay with a ground plane was first recognized by Bongianni[1] and later by Bardai, et al.[2] and Miller.[3] Figure 2 shows how, using two ground planes—one above and one below the YIG film, an increased operating bandwith results. A delay of about 95 ± 5 nS over a 400 MHz bandwidth was obtained for this device with an insertion loss of 20 dB.

Backward volume waves (BVW's) have shown linearly dispersive and constant delays as shown in Figure 3. In the upper curve a 15 μm YIG film was placed 150 μm from a ground plane to give a "down-chirp" dispersion linear to about ± 5 nS over an 800 MHz bandwidth. This delay line had a 20 dB insertion loss. The lower curve of Figure 3 was measured with a 20 μm film spaced about 10 μm or less from a ground plane. This configuration was achieved by placing the YIG film on a coplanar waveguide transducer. The close proximity of the ground plane to the YIG undoubtedly contributed to the higher insertion loss of 30 dB. As with the FVW delay line this BVW device gave a delay constant to within ± 5 nS over a 400 MHz bandwidth.

Finally, in Figure 4 are shown delay results for surface waves (SW's). Since SW's are unidirectional we differentiate between the +k and -k modes. Also SW's give smaller operating bandwidths than their volume wave counterparts even at S-band. In Figure 4 a 20 μm thick film was placed 250 μm from a ground plane using a 10 mil dielectric alumina wafer. For the -k waves we get a small but significant linear dispersion over a 350 MHz bandwidth. The insertion loss was 30 dB and resulted primarily because this -k wave was launched and received on the YIG film surface opposite to that of the transducers. The lower curve, for +k waves, shows a 200 MHz bandwidth of constant delay with an insertion loss of only 8 dB. This 8 dB figure was by no means a

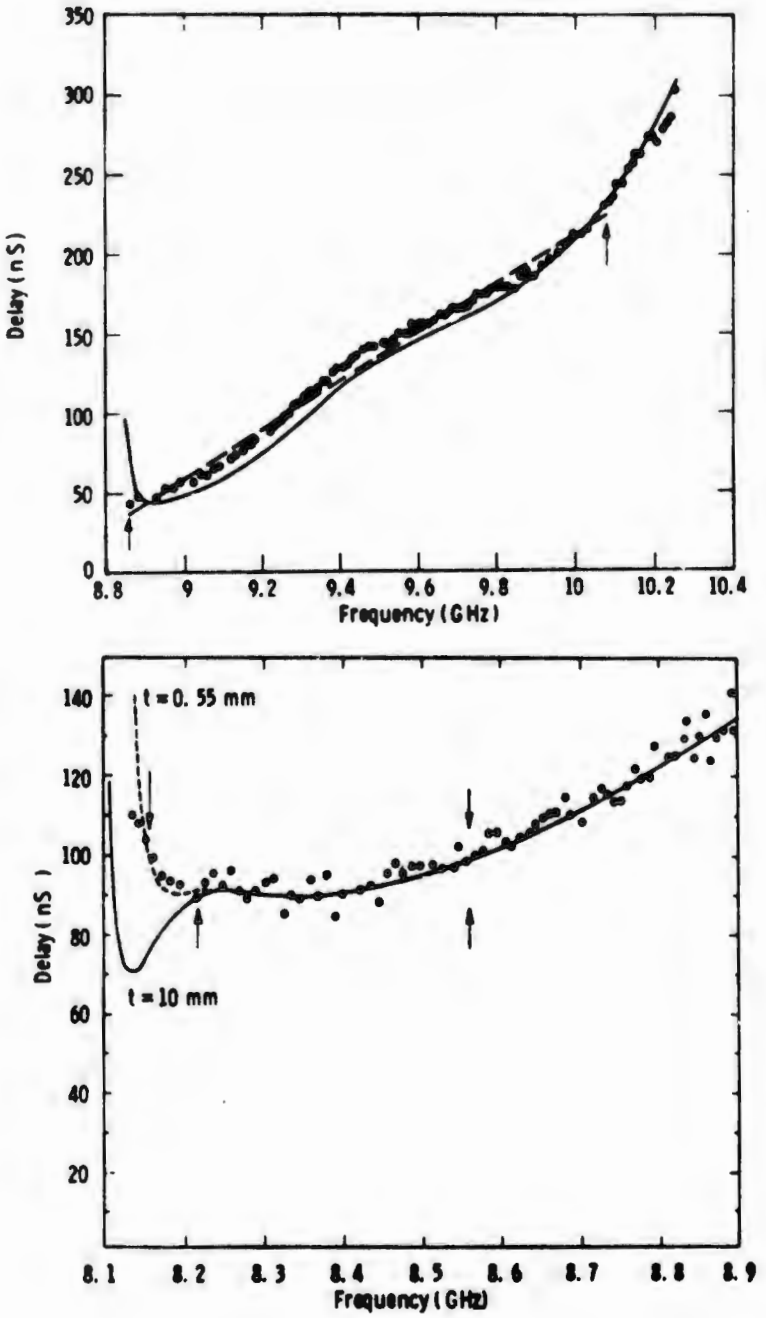

Figure 2. Upper: Delay versus frequency for a 20 μm thick film spaced 20 μm from a ground pland supporting forward volume waves. Lower: Delay versus frequency for a 20 μm thick film spaced 150 μm from an upper ground plane and (a) 10 mm (solid curve), (b) 0.55 mm (broken curve) from a lower ground plane. Dots are the experimentally measured values.

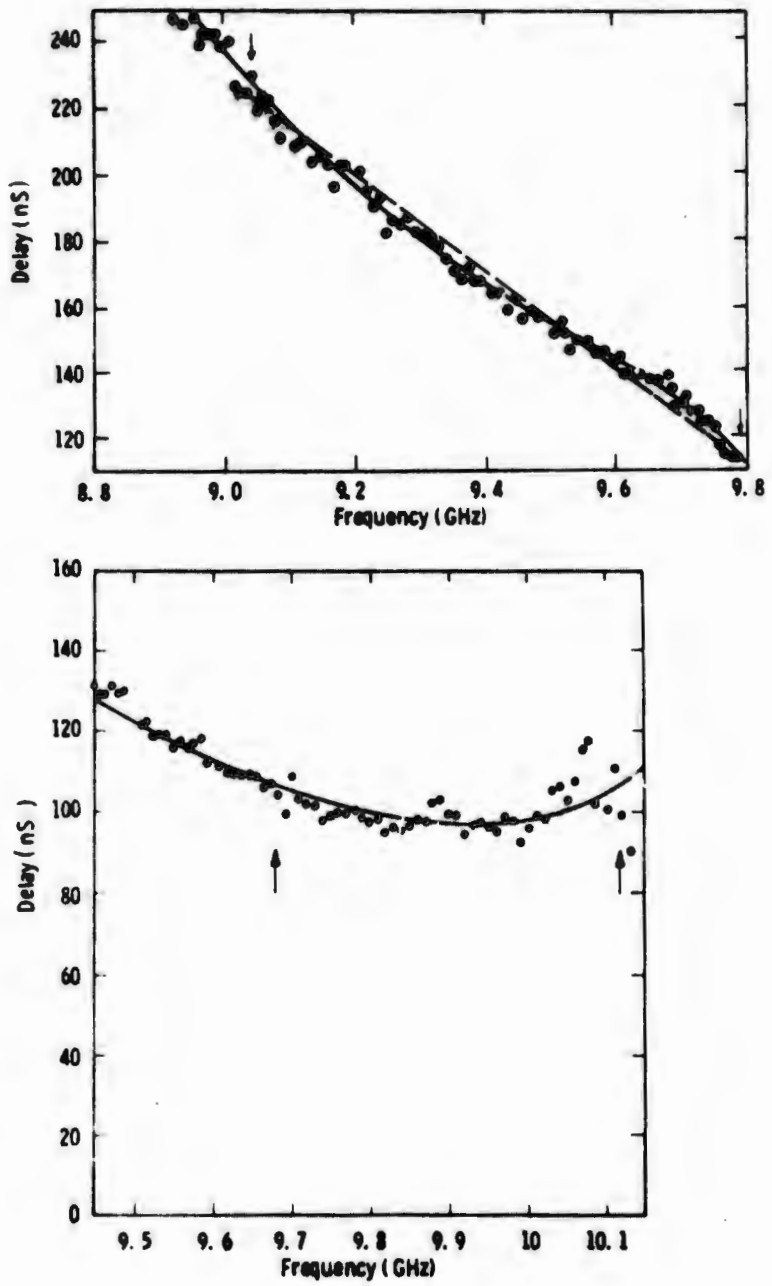

Figure 3. Upper: Delay versus frequency for a 15 μm thick film spaced 150 μm from a ground plane supporting backward volume waves. Lower: Delay versus frequency for 20 μm thick film spaced about 10 μm from a ground plane. Dots are the experimentally measured values.

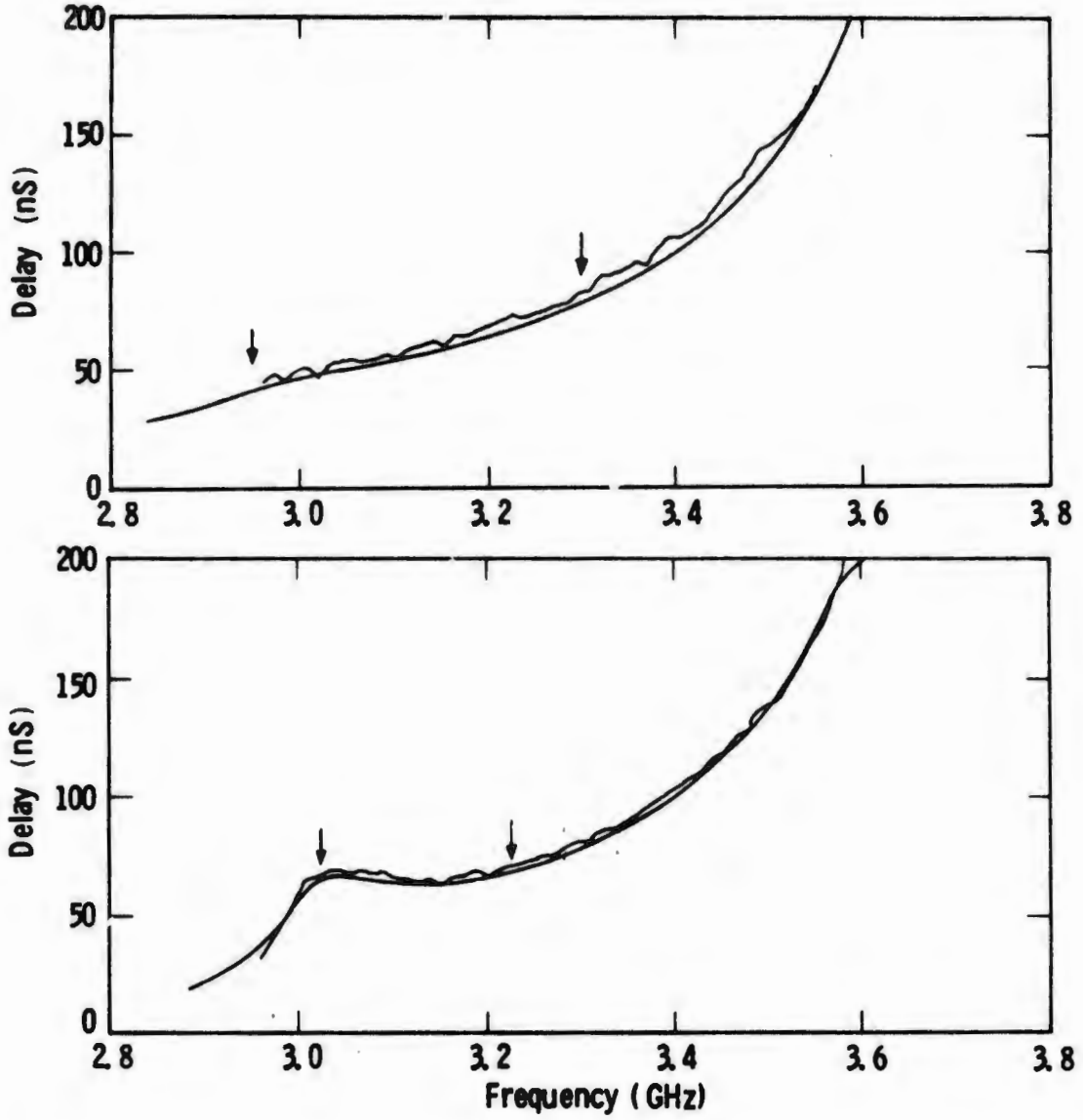

Figure 4. Upper: Delay versus frequency for a 20 μm thick film spaced 250 μm from a ground plane supporting -k surface waves. Lower: as above, except supporting +k surface waves. "Wiggly" curves are the experimental results.

lower limit. Because of the high coupling coefficient for SW's relative to volume waves plus the advantages of uni-directionality insertion losses of 3 dB or less may be anticipated with SW. The results were taken at S-band to exploit the increased bandwidth for SW's at the lowe microwave frequencies.

The calculated curves of Figures 2 through 4 were all done using the original approach of Damon and Eshbach[4] with allowance for ground plane boundaries and finite sample width. The only adjustable parameters used to get the agreement between theory and experiment to within 5 nS were the internal bias field H and the magnetization $4\pi M$. The bias field was uncertain to the extent of having no exact knowledge of the internal anisotropy field H_A. H_A was typically in the range 10 to 100 Oersteds depending on the orientation of H. $4\pi M$ can depend on crystal growth conditions — it being typically in the range 1750 to 1800 Gauss.

The characteristics of the simple delay lines described here are probably not sufficiently well controlled to permit their immediate use in say microscan receiver applications or phased array radars without some technique to reduce the residual delay ripple. A sensitive and frequently quoted parameter to describe the delay ripple tolerance is the phase deviation or error over the operating bandwidth. Microscan receiver applications call typically for a limit of 20° phase deviation from quadratic for the dispersive delay lines whereas some phased array radar requirements will only tolerate a 2° phase error from linearity for the constant delay lines. Figure 5 is a calculation of the quadratic phase error for the FVW dispersive delay line of Figure 2. The delay data over a 1 GHz bandwidth were fitted to a least squares straight line. The phase deviation ($\Delta\phi$) from this straight line is shown in Figure 5 and shows $\Delta\phi_{max} = \pm 100°$. Thus, without correction, the dispersive delay line has a phase error within a factor of 5 of that required by the microscan receiver for example.

A constant but adjustable delay can be obtained from "up-chirp"

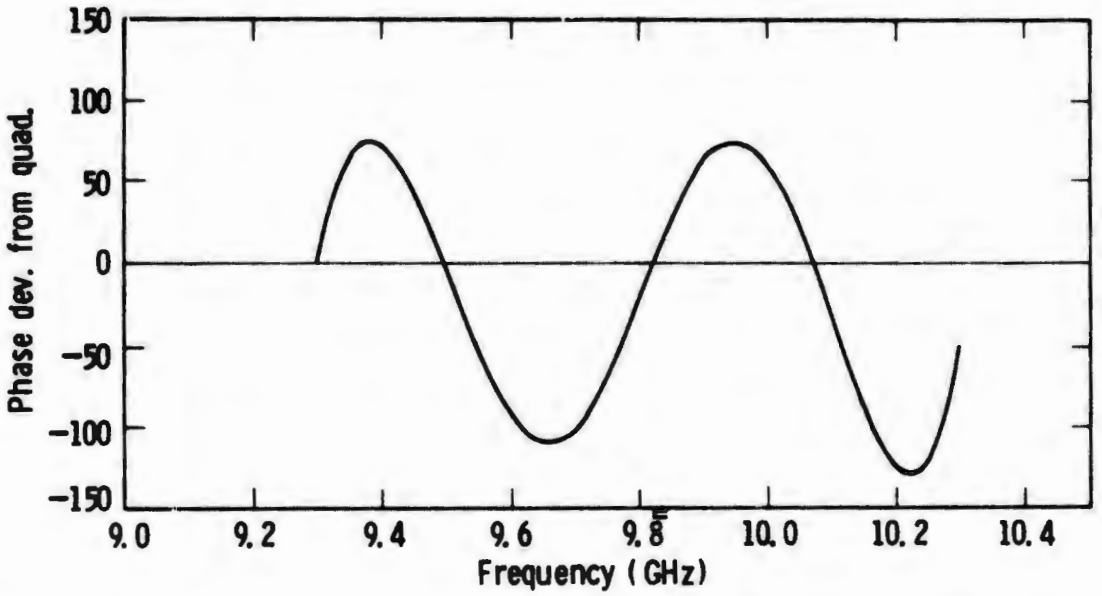

Figure 5. Phase deviation from ideal quadratic response versus frequency for the forward volume wave curve of Figure 2 (upper).

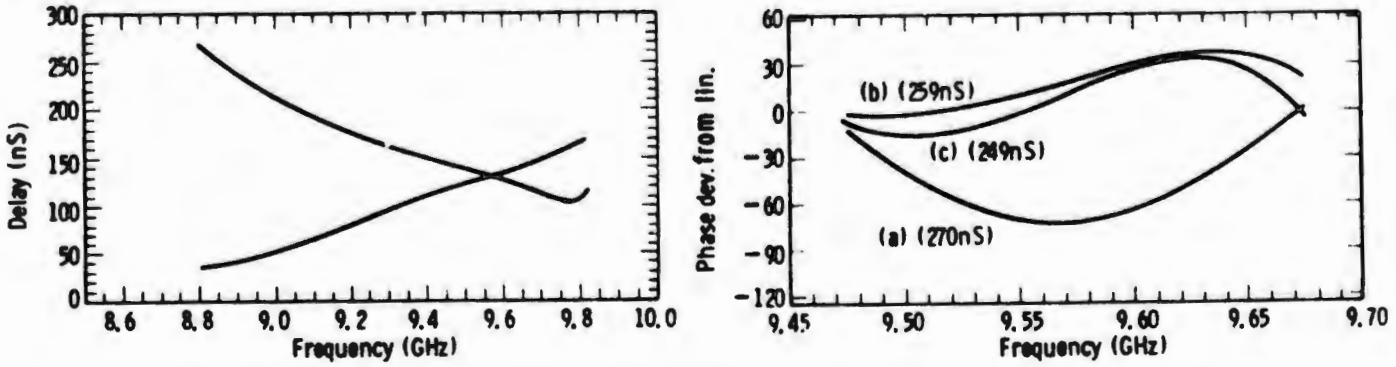

Figure 6. Left: Calculated delay responses versus frequency for the forward volume and backward volume curves shown in Figures 2 (upper) and 3 (upper). Right: Phase deviation from linearity versus frequency for the combined delay results of the upper curves, (a) FVW bias field 3041 Oe, (b) 3071 Oe, (c) 3101 Oe.

and "down-chirp" dispersive delay lines in series. Changing the bias field of, say, the "up-chirp" line slides its delay along the frequency axis causing the constant total delay to move up or down. In Figure 6 we show a calculation for the FVW and BVW delay lines. The lower curve shows, in terms of the phase error, how constant such a combined delay would be for ± 10 nS increments in delay adjustment. The calculation was done for 200 MHz of bandwidth with the most linear portions of the FVW and BVW curves. It gives another illustration of where these simple delay lines presently stand in terms of performance.

There are a number of possible techniques which could correct the second order delay ripple and in conclusion and as an illustration of one of these we show the effect of a small linear gradient (6%) in the bias field. Figure 7 (upper curve) is the same type of plot as Figure 5 except that the actual delay ripple is plotted rather than $\Delta\phi$. The lower curve shows that a 6% linear gradient in H over the path length of the delay line shifts the delay response down in frequency and away from the original least-squares fit straight line. However, substantial reduction in delay ripple does result but over a reduced bandwidth of about 500 MHz. A field gradient in H may not be the best solution to the delay ripple problem but it does illustrate that future developments and improvements can be expected in the performance of simple single transducer magnetostatic delay lines.

3. CONCLUSION

In conclusion, we have shown how both constant and linearly dispersive magnetostatic delay lines may be designed using single finger transducers which avoid the multiple reflection effects associated with

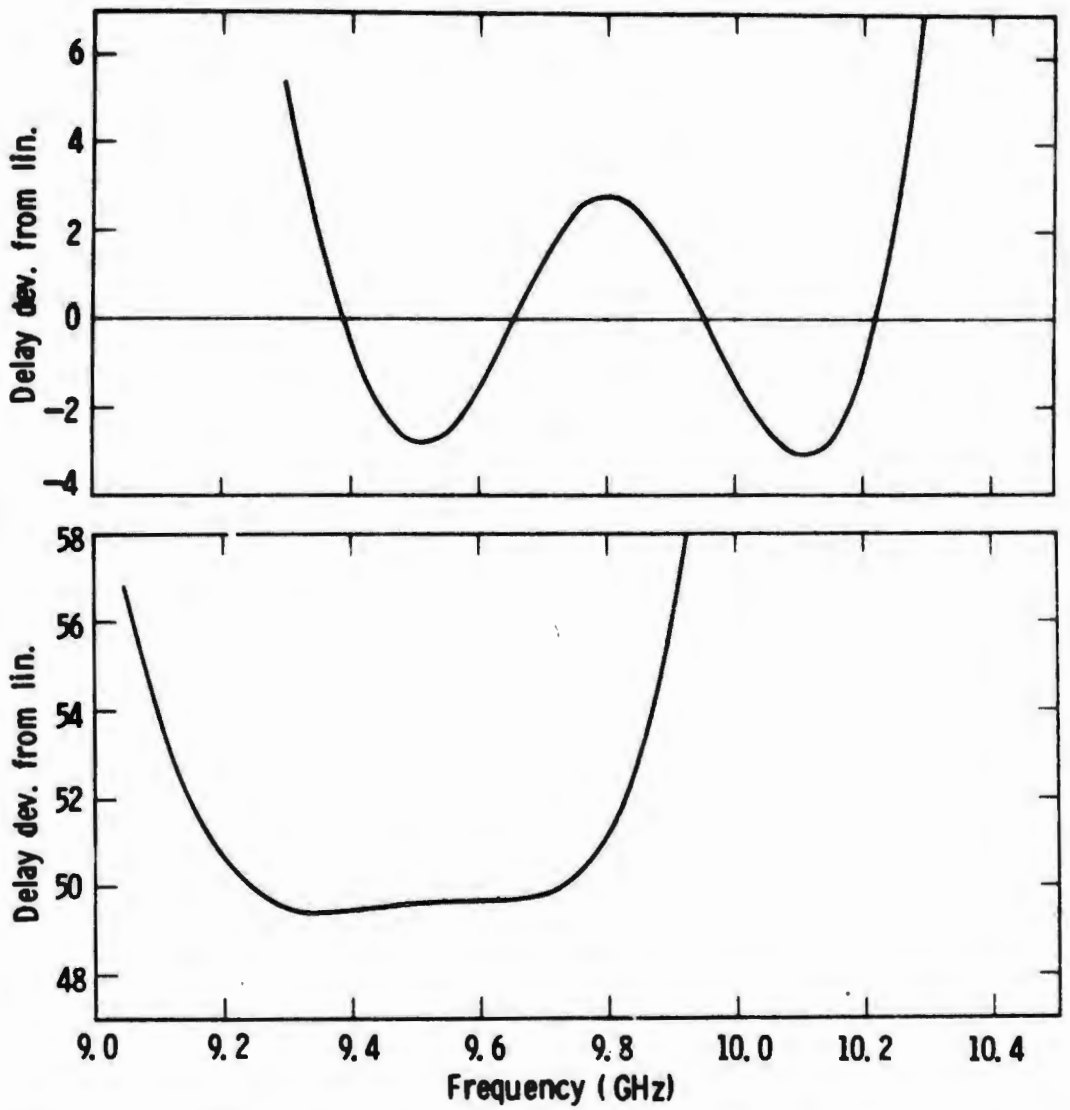

Figure 7. Upper: calculated delay ripple versus frequency for the FVW dispersive delay of Figure 2 (upper). Lower: Effect of a 6% linear bias field gradient along the path length of the FVW dispersive delay line.

interdigital or reflective array transducers. The desired delay characteristics were obtained through modification of the magnetostatic dispersion by one or more close proximity ground planes. The limitations of this approach in terms of delay ripple or phase error were shown.

Finally, an example of how the delay ripple might be reduced through a gradient in the bias field was given. At present, it is not known how to reduce the increased insertion loss which results from finite conductivity damping of the magnetostatic wave by the ground plane. This effect is more noticeable in the FVW dispersive delay line and the BVW constant delay line.

REFERENCES

1. W. L. Bongianni, J. Appl. Phys., 43, 2541 (1972).
2. Z. M. Bardai, J. D. Adam, J. H. Collins and J. P. Parekh, Magnetism and Magnetic Materials AIP Conf. Proc. No. 34, 268 (1977).
3. N. D. J. Miller, Phys. Stat. Solidi, (a) 37, 83 (1976).
4. R. W. Daman and J. R. Eshbach, J. Chem. Phys. Solidi, 9, 308 (1960).